Mapping color fluctuations in the photon in ultraperipheral heavy ion collisions at the Large Hadron Collider

M. Alvioli,[1] L. Frankfurt,[2,3] V. Guzey,[4] M. Strikman,[3] and M. Zhalov[4]

[1] *Consiglio Nazionale delle Ricerche, Istituto di Ricerca per la Protezione Idrogeologica, via Madonna Alta 126, I-06128 Perugia, Italy*
[2] *Particle Physics Department, School of Physics and Astronomy, Tel Aviv University, 69978 Tel Aviv, Israel*
[3] *Department of Physics, the Pennsylvania State University, State College, PA 16802, USA*
[4] *National Research Center "Kurchatov Institute", Petersburg Nuclear Physics Institute (PNPI), Gatchina, 188300, Russia*

arXiv:1605.06606v2 [hep-ph] 15 Mar 2017

We model effects of color fluctuations (CFs) in the light-cone photon wave function and for the first time make predictions for the distribution over the number of wounded nucleons ν in the inelastic photon–nucleus scattering. We show that CFs lead to a dramatic enhancement of this distribution at $\nu = 1$ and large $\nu > 10$. We also study the implications of different scales and CFs in the photon wave function on the total transverse energy ΣE_T and other observables in inelastic γA scattering with different triggers. Our predictions can be tested in proton–nucleus and nucleus–nucleus ultraperipheral collisions at the LHC and will help to map CFs, whose first indications have already been observed at the LHC.

I. INTRODUCTION

One of key features of high energy processes in the target rest frame is that the wave function of a projectile is the superposition of coherent (so-called frozen) configurations [1, 2], which is a consequence of the uncertainty principle and Lorentz slowing down of the interaction time. In the pre-QCD times, coherence of high energy processes has been extensively studied in the photon–nucleon (γN) and photon–nucleus (γA) collisions, for a review, see [3]. In particular, it was established that the resolved photon is dominated by the contribution of the light vector meson component of the photon wave function, which is responsible for about 70% of $\sigma_{\rm tot}(\gamma N)$. The origin of the photon components, which are responsible for the remaining 30% of the γN cross section, is a matter of debate.

In QCD coherence of high energy processes is well understood theoretically and established experimentally, for a review, see, e.g. [4, 5]. A distinctive feature of the QCD dynamics is that the interaction strength of different configurations of quarks and gluons, which are QCD constituents of projectile hadrons, photons, etc., varies. We refer to this phenomenon as color fluctuations (CFs). In the literature one alternatively uses the term cross section fluctuations, which refer predominantly to soft hadron (photon) interactions at high energies.

A particular dramatic example of CFs is the phenomenon of color transparency (CT) when, as a consequence of color screening, the strength of the interaction of a high energy hadron (photon) in a configuration with a small transverse size is much smaller than the average interaction strength, for a recent review, see [6]. While CT is a natural mechanism for the interaction with the strength smaller than the average one, several mechanisms like fluctuations of transverse size, gluon density, the phenomenon of spontaneously broken chiral symmetry, etc. can contribute to fluctuations with the larger-than-average interaction strength.

It has been demonstrated long ago by the direct calculations that the contribution of planar diagrams to the total cross section of a hadron–hadron collision tends to zero with an increase of the collision energy [7]. Therefore, the contribution of consecutive multiple rescatterings of a hadron projectile to the total cross section of the hadron–nucleus scattering described by planar Feynman diagrams rapidly decreases with an increase of the invariant collision energy s [8]. Thus, within a quantum field theory multiple interactions of the projectile are dominated at high energies by the contribution of non-planar diagrams. The Gribov–Glauber approximation [1] has been suggested to resolve this theoretical puzzle. It accounts for the contribution of non-planar diagrams and employs duality between non-planar diagrams and a sum of the elastic contribution and the diffractive intermediate states (duality between s and t channels) to rewrite formulae in the form rather similar to the Glauber approximation [1]. This theoretical description accounts for coherence of high energy processes and predicts that the geometry of hA collisions should be rather close to that expected within the Glauber approach. Hence the Gribov–Glauber approximation is routinely used in the evaluation of geometry of the heavy ion collisions. By virtue of duality the Gribov–Glauber approximation includes diffractive intermediate states, which allow one to account for energy–momentum conservation, see the discussion in [9]. The presence in the formulae of the contribution of inelastic diffractive states leads to the inelastic shadowing correction for $\sigma_{tot}(pA)$ [8]. The inelastic shadowing correction was evaluated in a number of papers and found to agree well with the data, see discussion and references in, e.g., [10].

It has been suggested that the interaction matrix of the initial hadron or diffractively produced hadronic states with target nucleons, which arises within Gribov–Glauber approach, can be diagonalized [11, 12]. In the particular case,

when diffractive intermediate states are resonances, this diagonalization has been performed in [13]. The method of CFs developed in [14] and discussed below is the further generalization of the Gribov–Glauber approximation, which allows one to account for the fluctuations of the interaction strength and other implications of QCD.

Several effects were observed at collider energies, which naturally emerge in the CF framework. First, the ATLAS study [15] of the charged-particle pseudorapidity distribution $dN_{\rm ch}/d\eta$ in proton–lead (pPb) collisions at $\sqrt{s_{NN}} = 5.02$ TeV as a function of centrality and the pseudorapidity η showed that CFs affect the collision geometry by broadening the distribution of the number of participating nucleons $N_{\rm part}$ for large $N_{\rm part}$ (Fig. 13 of Ref. [15]). It can be interpreted as broadening of the distribution in the number of wounded nucleons naturally emerging in the CF approach [14] (note that in these early papers, CFs were called cross section fluctuations). It results in a milder dependence of $dN_{\rm ch}/d\eta(\langle N_{\rm part}\rangle/2)$ on centrality, especially at large negative rapidities in the Pb-going direction (Figs. 11 and 12 of Ref. [15]) than that expected in the combinatorics of the geometric Gribov–Glauber model [16]. The numerical results for the distribution of CFs in the proton used in the analysis of [15] are consistent with the expectations of [17, 18].

The second effect is the observation of a large violation of the Gribov–Glauber approximation for the dependence of the jet production on the centrality observed in pA collisions at the LHC [19] and in dA collisions at RHIC [20], for which a large-x parton momentum fraction of the proton is involved. The central-to-peripheral $R_{\rm CP}$ ratio is suppressed by as much as 80% at the LHC and 50% at RHIC at the largest measured p_T. At the same time the combinatorics given by the geometric Glauber picture works very well for the collisions with up to eight nucleons, if x is small enough, $x \leq 0.1$. While CFs only increase the deviation of $R_{\rm CP}$ from unity, this pattern is consistent with the x-dependence of CFs expected within QCD [21].

The third effect is the significant suppression of the rate of ρ meson production in the coherent $\gamma A \to \rho A$ reaction measured in Pb-Pb ultraperipheral collisions (UPCs) at the LHC [22] as compared to the expectations of the vector dominance model combined with the Gribov–Glauber approximation for the photon–nucleus interaction. This was explained in [23] by taking into account the effect of CFs in the photon wave function, which reduce the effective ρ–nucleon cross section by suppressing the overlap of the vector meson and photon wave functions and lead to sizable inelastic (Gribov) nuclear shadowing due to the photon inelastic diffraction into large masses.

In this paper we argue that one can map CFs in the photon wave function using ultraperipheral collisions (UPCs) of heavy ions at the LHC. Although feasibility of UPC studies was analyzed at length in [24], the studies discussed below were not addressed. Primarily this is because such analyses became feasible due to the experience accumulated in the analysis of pA collisions at the LHC. In a long run studies along these lines at the Electron-Ion Collider [25, 26] would provide a detailed information on CFs in the photon and their dependence on the photon virtuality. The main challenge for building a realistic description of the photon–nucleon (nucleus) interactions at collider energies is to take into account the multi-scale structure of the light-cone wave function of the photon associated with presence of soft and hard intrinsic scales. In particular, the photon wave function contains several types of configurations: large-σ configurations characterized by small transverse momenta $k_t < 0.5$ GeV and invariant masses comparable to the masses of light vector mesons interacting with the strength $\sim \sigma_{\pi N}$ ($\sigma_{\pi N}$ is the total pion–nucleon cross section), configurations interacting with σ much larger than $\sigma_{\pi N}$ related to the presence of soft large-mass diffraction, and small-σ configurations with large $k_t \geq 1$ GeV, whose contribution results in the leading twist nuclear shadowing. UPCs at the LHC correspond to a wide interval of invariant energies $W \leq 500$ GeV, where hard physics should be well described within the DGLAP approximation, see [27] and references therein. Thus, a more rapid increase of parton distributions with energy at extremely small x, which is often discussed in the literature, is beyond the scope of this paper.

We propose a model of CFs in the hadronic component of the photon wave function by combining the information obtained in the analysis of photoproduction of ρ mesons at the LHC energies [23], which enables us to model the photon configurations interacting mostly with the strength exceeding the typical ρ–nucleon cross section, with that obtained in photoproduction of J/ψ mesons [28], which is amenable to the perturbative QCD (pQCD) description of the weakly-interacting configurations. Since the information on coherent photoproduction of ρ and J/ψ is available for $W \sim 100$ GeV, we focus in this paper on this energy range. The W dependence of the discussed effects for higher W will be considered elsewhere.

We apply the resulting model of the photon CFs to the calculation of the distribution over the number of wounded nucleons, ν, involved in the inelastic γA scattering. We show that as a consequence of CFs around the average value, the soft inelastic nuclear shadowing effect is strongly enhanced as compared to pA collisions. We also take into account an additional effect of the different pattern of the interaction of small dipoles, which leads to the leading twist nuclear shadowing and which is absent in the Gribov–Glauber approximation. This effect leads to the significant probability for small dipoles to interact with several nucleons, which noticeably reduces the distribution over ν for small values of ν.

This paper is organized as follows. In Sect. II we develop a model for CFs in the photon wave function for the photon–nucleon interaction. In Sect. III we present and discuss our predictions for the distribution over the number of wounded nucleons (inelastic interactions) in the inelastic photon–nucleus scattering. In the calculations we use our

model for CFs in the photon without and with an additional effect of the leading twist nuclear shadowing for the configurations interacting with small cross sections. In Sect. IV, we make a prediction for the transverse energy $\sum E_T$ distribution in γA collisions using as a starting point the model of [15] for the dependence of $\sum E_T$ on ν. Finally, in Sect. V we discuss possibilities of special triggers, which would allow one to use γA scattering to map out different components of the photon wave function.

II. COLOR FLUCTUATIONS IN γA SCATTERING: GENERAL FORMALISM

At sufficiently high photon energies E_γ in the target rest frame, the coherence length associated with the hadronic fluctuation (component) of the photon wave function of mass M exceeds the target radius R_T, $l_{\rm coh} = 2E_\gamma/M^2 > R_T$. In this case, the forward photon–target amplitude (the total photoabsorption cross section) can be expressed in terms of the dispersion representation over the masses M^2 [29]:

$$\sigma_{\gamma N} = \frac{\alpha_{\rm e.m.}}{24\pi^2}\int \frac{dM^2}{M^2} R_{e^+e^-\to {\rm hadrons}}(M^2)\sigma_{MN}\,, \tag{1}$$

where $\alpha_{\rm e.m.}$ is the fine structure constant; $R_{e^+e^-\to {\rm hadrons}}(M^2) = \sigma(e^+e^-\to {\rm hadrons})/\sigma(e^+e^-\to \mu^+\mu^-)$ is the ratio of the e^+e^- annihilation cross sections into hadrons (everything) and a muon pair, respectively, of a given invariant mass squared M^2; σ_{MN} is the total cross section for the interaction of a given component with the target. It is important to emphasize that non-diagonal transitions between different photon components have been neglected in Eq. (1), which can be justified at present in the case of a heavy nuclear target [29].

In the vector meson dominance model (VMD), 70% of the integral in Eq. (1) is due to the sum of ρ, ω and ϕ mesons, which interact with hadrons with a strength similar to that of a pion (for ρ and ω) [3, 30, 31].

A straightforward generalization of Eq. (1) to the case of deep inelastic scattering (DIS) leads to a gross violation of the approximate Bjorken scaling, and hence to the contradiction with the leading twist QCD expectations. In the framework of the parton model, the qualitative resolution of the paradox was suggested by Bjorken [32] by assuming that the interaction is dominated by the so-called aligned quark–antiquark pairs, where the quarks share asymmetrically the photon longitudinal momentum and have small transverse momenta p_t. Such aligned quark–antiquark pairs configurations are strongly interacting with a nuclear target and correspond to typical vector meson-like (and/or other hadronic) configurations. Their contribution to the total virtual photon–nucleon cross section $\sigma_{\gamma^* N}$ is suppressed by a factor of μ^2/M^2, where μ is a soft QCD scale, which leads to the scaling of $\sigma_{\gamma^* N}$.

In QCD the situation is somewhat different [33]: in addition to the aligned pairs, configurations with large p_t also contribute to $\sigma_{\gamma^* N}$; their noticeable contribution is proportional to $\alpha_s(p_t^2)/p_t^2$, where α_s is the strong coupling constant, and grows with an increase of the collision energy.

Overall this leads to the following approximate picture of the hadronic component of the wave function of the photon: the majority of the configurations interact with strengths similar to the one given by CFs in the $\gamma\to\rho,\omega$ transitions; they dominate at large and medium $\sigma \geq \sigma_{\pi N}$. (They also include the fluctuations in the aligned jet component.) Note that with an increase of collision energies, these configurations are likely to be somewhat more localized than those in the elastic vector meson–nucleon scattering [23]. In addition, there is a component which dominates for small σ and which is described by the perturbative (dipole) wave function interacting with the strength given by perturbative QCD.

The formalism of cross section fluctuations was introduced before advent of QCD to explain presence of inelastic diffraction at small t [11, 12]. Its connection to the Gribov inelastic shadowing for double scattering was pointed out in [34]. The basic idea of this approach is to diagonalize the interaction matrix which arises in the Gribov–Glauber approach in the basis of elastic and diffractive states. The obtained matrix describes the distribution over the values of the cross section. If diffractive states are hadron resonances, this program can be effectively performed [13]. It was possible to extend this formalism by accounting for the well understood QCD phenomena to reconstruct the form of the distribution $P_\gamma(\sigma, W)$ [13, 35], where W is the invariant photon–proton energy. While the form of $P_\gamma(\sigma, W)$ can be calculated from the first principles only for small σ [36], it can be constrained by the following integral relations:

$$\begin{aligned}\int d\sigma P_\gamma(\sigma,W)\sigma &\equiv \langle\sigma\rangle = \sigma_{\gamma p}(W)\,,\\ \int d\sigma P_\gamma(\sigma,W)\sigma^2 &\equiv \langle\sigma^2\rangle = 16\pi\frac{d\sigma_{\gamma p\to Xp}(W,t=0)}{dt}\,,\end{aligned} \tag{2}$$

where $\sigma_{\gamma p}(W)$ is the total photon–nucleon cross section; $d\sigma_{\gamma p\to Xp}(W,t=0)/dt$ is the cross section of photon diffractive dissociation on the proton including the ρ meson peak, which determines the dispersion of CFs encoded in $P_\gamma(\sigma, W)$.

Note that the distribution $P_\gamma(\sigma, W)$ is not normalizable [36], i.e., the integral $\int d\sigma P_\gamma(\sigma, W)$ is divergent at the lower integration limit due to the infinite renormalization of the photon Green's function (the vacuum polarization).

Therefore, to model CFs in the photon, we build a model interpolating between the regimes of small and large σ. For the former, we use the color dipole model (CDM) of the photon wave function, where the (usually virtual) photon is treated as superposition of quark–antiquark pairs (dipoles). The dipoles interact with the target with cross sections given by the factorization theorem of perturbative QCD for small dipoles [38]. Note that in the literature there is a popular assumption that the contribution of light vector mesons to the photon–nucleon cross section is dual to the integral over the small masses of $q\bar{q}$ pairs (for example, $M^2 \leq 1$ GeV^2 for ρ, ω-mesons). The CDM gives a reasonable description of CFs for $\sigma \ll \sigma(\pi N)$. For large σ, $\sigma \gg \sigma(\pi N)$, the CFs are determined by non-perturbative effects both in terms of the photon configurations involved and the strength of the interaction. Therefore, we use the modified VMD (mVMD) approach [23] to model their effects.

In our analysis we use the results of the approach developed in [37], which gives a good description of the proton structure function $F_{2p}(x, Q^2)$ down to $Q^2 \sim 0.3$ GeV^2. In this approach, the dipole cross section $\sigma_{q\bar{q}}$ is built in a piece-wise form. For small dipoles corresponding approximately to $d_t \leq 0.3 - 0.4$ fm, one has [38]:

$$\sigma_{q\bar{q}}(W, d_t, m_q) = \frac{\pi^2}{3} d_t^2 \alpha_s(Q^2_{\rm eff}) x_{\rm eff} g(x_{\rm eff}, Q^2_{\rm eff}) \,, \tag{3}$$

where W is the invariant photon–nucleon center of mass energy, $Q^2_{\rm eff} = \lambda/d_t^2$ for light quarks and $Q^2_{\rm eff} = m_q^2 + \lambda/d_t^2$ for heavy quarks; $x_{\rm eff} = 4m_q^2/W^2 + 0.75\lambda/(W^2 d_t^2)$; $m_q = 300$ MeV for light u, d and s quarks and $m_c = 1.5$ GeV. This choice of the quark masses ensures that the average transverse size of $q\bar{q}$ configurations in the photon wave function is close to that of the pion, $d_\pi = 0.65$ fm, and also leads to a smoother interpolation between small and large σ regimes. The parameter $\lambda = 4$ is chosen to best reproduce the HERA data on diffractive J/ψ photoproduction [39]. Note, however, that heavy quarks give a very small contribution to the quantities we discuss below.

For large dipole sizes, $\sigma_{q\bar{q}}$ is constrained to be equal to the total pion-nucleon cross section at the appropriate energy at $d_t = d_\pi = 0.65$ fm and to slowly grow for $d_t > 0.65$ fm. Finally, for the intermediate values of $0.3 - 0.4 < d_t < 0.65$ fm, $\sigma_{q\bar{q}}$ is modeled as a smooth interpolation between the low-$\sigma_{q\bar{q}}$ (3) and large-$\sigma_{q\bar{q}}$ limits.

As a result, one can write the interpolation formula for $\sigma_{\gamma p}(W)$ as

$$\sigma_{\gamma p}(W) = \sum_q e_q^2 \int dz\, d^2 d_t \sigma_{q\bar{q}}(W, d_t, m_q) |\Psi_{\gamma,T}(z, d_t, m_q)|^2 \,, \tag{4}$$

where z is the fraction of photon momentum carried by the quark in the dipole; d_t is the transverse distance between the quark and the antiquark; e_q are the quark charge. The photon wave function squared in the mixed momentum–coordinate representation is given in [40].

It is worth emphasizing here that the dominant contribution to $\sigma_{\gamma p}$ in Eq. (4) originates from the nonperturbative interactions of large-size multiparton hadron-like configurations in the photon wave function, which do not resemble $q\bar{q}$ dipoles. Duality considerations suggest that the contribution of such configurations can be approximated using the lightest vector meson. Hence, we first calculate P_γ in the model of Eq. (4) and next match it at moderate σ to the nonperturbative model for CFs for transitions to light mesons.

Since $\sigma_{\gamma p}(W) = \int d\sigma \sigma P_\gamma(\sigma, W)$, one finds within the model of Eq. (4):

$$P_\gamma^{\rm dipole}(\sigma, W) = \sum_q e_q^2 \left| \frac{\pi d d_t^2}{d\sigma_{q\bar{q}}(W, d_t, m_q)} \right| \int dz |\Psi_{\gamma,T}(z, d_t(\sigma_{q\bar{q}}), m_q)|^2 \Big|_{\sigma_{q\bar{q}}(W, d_t, m_q) = \sigma} \,. \tag{5}$$

Note that the right-hand side of (5) is expressed in terms of $\sigma_{q\bar{q}}(W, d_t, m_q)$, which is then identified with σ. The resulting distribution $P_\gamma^{\rm dipole}(\sigma, W)$ as a function of σ for different light quark masses m_q and at $W = 100$ GeV is shown by the green dashed curves. To examine the sensitivity of $P_\gamma^{\rm dipole}(\sigma, W)$ to the choice m_q, we varied the light quark mass in the interval $0 \leq m_q < 350$ MeV; the results are shown in Fig. 1, where the dashed curves from the upper to the lower one correspond to $m_q = 0$, $m_q = 250$ MeV, $m_q = 300$, and $m_q = 350$ MeV, respectively.

Since in the used model the $\sigma(q\bar{q}N)$ cross section does not exceed approximately 40 mb, the resulting distribution $P_\gamma^{\rm dipole}(\sigma, W)$ of Eq. (5) has support only for $0 \leq \sigma \leq 40$ mb.

For large σ, the distribution $P_\gamma(\sigma, W)$ can be well approximated by the distribution $P(\sigma)$ for the $\gamma \to \rho$ transition. Taking the sum of the ρ, ω and ϕ meson contributions, the resulting distribution reads:

$$P_{(\rho+\omega+\phi)/\gamma}(\sigma, W) = \frac{11}{9} \left(\frac{e}{f_\rho} \right)^2 P(\sigma, W) \,, \tag{6}$$

where $P(\sigma, W)$ is taken from [23]; the coefficient of 11/9 takes into account the ω and ϕ contributions in the SU(3) approximation (which somewhat overestimates the rather small contribution of ϕ mesons). The form of $P(\sigma, W)$ is motivated by $P_\pi(\sigma, W)$ for the pion and takes into account presence of the large-mass diffraction at high energies. It is also constrained to describe the HERA data on ρ photoproduction on the proton, which requires to account for a suppression of the overlap of the photon and ρ wave function as compared to the diagonal case of the $\rho \to \rho$ transition.

The resulting $P_{(\rho+\omega+\phi)/\gamma}(\sigma)$ at $W = 100$ GeV is shown by the blue dot-dashed curve in Fig. 1.

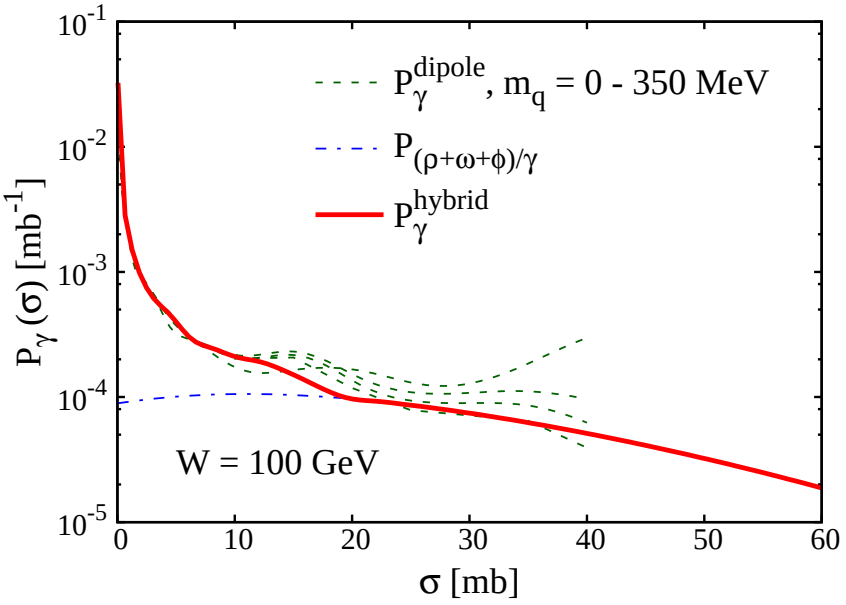

FIG. 1: The distributions $P_\gamma(\sigma, W)$ for the photon at $W = 100$ GeV. The red solid curve shows the full result of the hybrid model, see Eq. (7). The green dashed and blue dot-dashed curves show separately the dipole model and the vector meson contributions evaluated using Eqs. (5) and (6), respectively.

We build a hybrid model of $P_\gamma(\sigma, W)$ by interpolating between the regime of small $\sigma \leq 10$ mb, where perturbative dipole approximation is applicable and there is no dependence on the light quark mass m_q, and the regime of large σ, where the soft contribution due to the lightest vector meson dominates (hence we neglect the soft contribution of configurations with the large mass and small k_t). In particular, in our analysis we use the following expression:

$$P_\gamma(\sigma, W) = \begin{cases} P_\gamma^{\rm dipole}(\sigma, W)\,, & \sigma \leq 10 \text{ mb}\,, \\ P_{\rm int}(\sigma, W)\,, & 10 \text{ mb} \leq \sigma \leq 20 \text{ mb}\,, \\ P_{(\rho+\omega+\phi)/\gamma}(\sigma, W)\,, & \sigma \geq 20 \text{ mb}\,. \end{cases} \tag{7}$$

where $P_{\rm int}(\sigma)$ is a smooth interpolating function. The resulting $P_\gamma(\sigma, W)$ is shown by the red solid curve in Fig. 1.

Our model for $P_\gamma(\sigma, W)$ satisfies the constraints of Eq. (2) and gives the good description of the total and diffraction dissociation photon–proton cross sections at $W = 100$ GeV. Indeed, for $\sigma_{\gamma p}$, we obtain $\int_0^{100\text{ mb}} d\sigma \sigma P_\gamma(\sigma, W) = 135$ μb, which agrees with the PDG value of $\sigma_{\gamma p} = 146$ μb [41]. For the cross section of diffractive dissociation, we obtain $\int_0^{100\text{ mb}} d\sigma \sigma^2 P_\gamma(\sigma, W)/(16\pi) = 240$ μb/GeV^2. It agrees with our estimate of $d\sigma_{\gamma p \to Xp}(t = 0)/dt \approx 220$ μb/GeV^2, which is obtained by integrating the data of [42] over the produced diffractive masses and extrapolating the resulting cross section to the desired $W = 100$ GeV.

To quantify the width of CFs, one can introduce the dispersion ω_σ. For the photon, it can be introduced by the following relation:

$$\int d\sigma \sigma^2 P_\gamma(\sigma, W) = (1 + \omega_\sigma) \left(\frac{e}{f_\rho} \hat{\sigma}_{\rho N} \right)^2 , \tag{8}$$

where $\hat{\sigma}_{\rho N}$ is the ρ meson–nucleon cross section. The use of our $P_\gamma(\sigma, W)$ in Eq. (8) gives $\omega_\sigma \approx 0.93$, which should be compared to $\omega_\sigma^\rho \approx 0.54$ for the pure ρ meson contribution to $P_\gamma(\sigma, W)$ and to $\omega_\sigma^\pi \approx 0.45$ for CFs in the pion [35].

III. COLOR FLUCTUATIONS AND THE NUMBER OF WOUNDED NUCLEONS IN γA SCATTERING

One of important advantages of the Gribov–Glauber approximation is that it accounts for diffractive processes in the intermediate states including the photon diffraction into large masses and, therefore, conserves energy–momentum by virtue of duality between the parton model and hadronic descriptions. On the contrary, the Gribov–Glauber model, which accounts for elastic intermediate state only [16], violates energy–momentum conservation for the processes with multiple multiplicity of wound nucleons; it is proven by direct calculations of the energy released in such processes. A Monte-Carlo procedure including finite size effects in the elementary cross section and short-range correlations between nucleons was developed in [18]. Thus, the formulae for the number of wounded nucleons follow directly from the formulae for the CFs but differ from the combinatorics of the Glauber model due to the need to average over values of the cross section. For hard processes, nuclear shadowing and its impact on the number of wounded nucleons is calculated separately through the QCD factorization theorem.

It has been understood long ago that the large coherence length prevents cascading of rapid secondary hadrons since they are formed outside of a target. Thus, only low-energy cascades are allowed. Hence, the number of wounded nucleons given by the formulae below can be probed by selecting a kinematical region in the rapidity, where the contribution of cascades is expected to be small, see the discussion in the next section.

Previously we used the CF model to calculate the cross section of inelastic interactions with exactly ν nucleons, σ_ν, in pA collisions. The model was found to be consistent with the data at least up to $\nu \sim 10$ [15]. Hence it is natural to use a similar approach to account for the CF in the photon wave function in γA scattering for the interaction strength comparable or larger than $\sigma(\pi N)$ (CF effects due to the contribution of small-size configurations to be discussed later, see Eq. (11)). Then, for the photon–nucleus cross section corresponding to exactly ν inelastic interactions with the target nucleons, σ_ν, one obtains in the Gribov–Glauber model in the optical model limit:

$$\sigma_\nu = \int d\sigma P_\gamma(\sigma, W) \left(\begin{array}{c} A \\ \nu \end{array} \right) \int d^2\vec{b} \left[\frac{\sigma_{in}(\sigma) T_A(b)}{A} \right]^\nu \left[1 - \frac{\sigma_{in}(\sigma) T_A(b)}{A} \right]^{A-\nu} , \tag{9}$$

where $\vec{b}$ is the impact parameter; σ_{in} is the inelastic, non-diffractive cross section for the configuration characterized by the total cross section σ; $T_A(b) = \int dz \rho_A(b,z)$ in the nuclear optical density, where $\rho_A(r)$ is the density of nucleons. Note that we use $\sigma_{in} = 0.85\,\sigma$ (it is based on our estimate that in the considered range, the elastic cross section constitutes approximately 15% of the total one) and the Wood–Saxon density of nucleons for the ^{208}Pb target [18] in our analysis. In the derivation of Eq. (9), we employ the discussed above equivalence between the Gribov–Glauber model and cross section fluctuations approach. This equivalence becomes trivial, if one uses the approximation of completeness over diffractively produced states. It is worth emphasizing that we consider here soft interaction of the multiparton configurations of the hadronic component of the photon wave function. For the interaction of the projectile consisting **exactly** of two constituents, only $\nu = 1, 2$ are allowed, see Ref. [7, 43].

The probability to have exactly ν wounded nucleons in γA scattering, $P(\nu)$, reads:

$$P(\nu, W) = \frac{\sigma_\nu}{\sum_1^\infty \sigma_\nu} , \tag{10}$$

where σ_ν are given by Eq. (9). The probability distribution $P(\nu, W)$ calculated using Eqs. (9) and (10) is shown in Fig. 2 by the curve labeled "Color Fluctuations". For comparison, we also show the results of the calculation, where the effect of CFs is neglected and the photon is represented by an effective fluctuation interacting with the total cross section $\sigma = 25$ mb; the corresponding curve is labeled "Glauber".

Equation (9) does not take into account that in QCD, configurations corresponding to a small cross section of the interaction with the nucleon at high energies interact with the collective small-x gluon field of the nucleus, which is suppressed compared to the sum of the individual gluon fields of the nucleons due to the phenomenon of the leading twist (LT) nuclear shadowing [44]. This is supported by the observation of the large LT shadowing in coherent photoproduction of J/ψ in Pb-Pb UPCs at the LHC [45–47]. This implies that Eq. (9) underestimates the probability of the interaction with two and more nucleons for small σ, which is determined by the LT nuclear shadowing. It effectively takes into account the implication of QCD factorization theorem: the presence of the multiparton configurations in a small size $q\bar{q}$ configurations which are ignored in the eikonal models and in particular in Eq. (9).

To take into the account this effect, we modify Eq. (9) and use the following expression:

$$\sigma_\nu = \int_0^\infty d\sigma P_\gamma(\sigma, W) \left(\begin{array}{c} A \\ \nu \end{array} \right) \left[\frac{\sigma^{in}}{\sigma^{in}_{\rm eff}} \Theta(\sigma_0 - \sigma) + \Theta(\sigma - \sigma_0) \right] \int d^2\vec{b} \left[\frac{\sigma^{in}_{\rm eff} T_A(b)}{A} \right]^\nu \left[1 - \frac{\sigma^{in}_{\rm eff} T_A(b)}{A} \right]^{A-\nu} , \tag{11}$$

where $\sigma_0 = 20$ mb (see details below); $\sigma^{in}/\sigma^{in}_{\rm eff} \approx \sigma/\sigma_{\rm eff} < 1$ is the suppression factor modeling the effect of the LT shadowing. The effective cross section of $\sigma_{\rm eff}$ (note that $\sigma^{in}_{\rm eff} = 0.85\sigma_{\rm eff}$) is a function of σ, which we determine

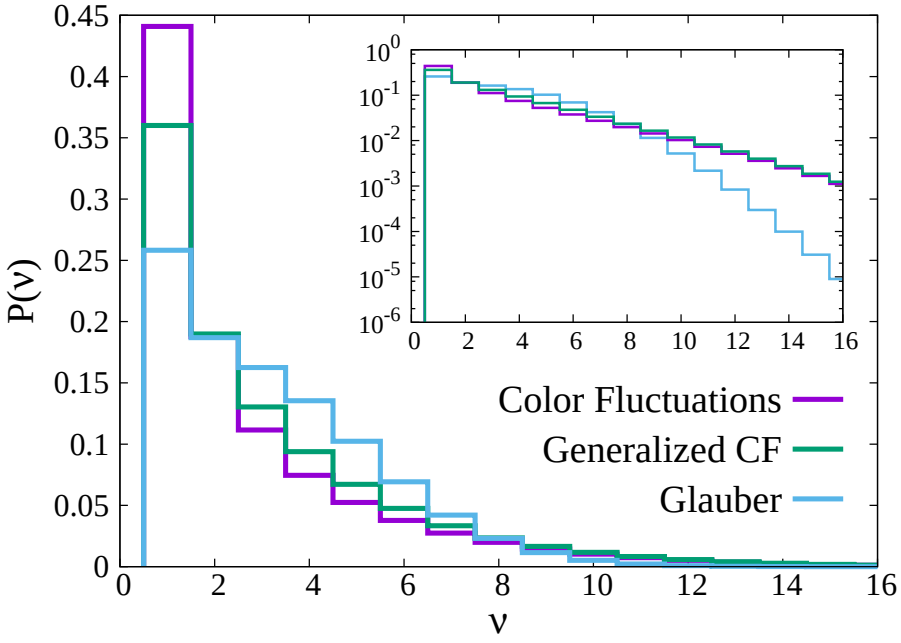

FIG. 2: The probability distributions $P(\nu, W)$ of the number of inelastic collisions ν. Predictions of Eqs. (9) and (11) are shown by the curves labeled "Color Fluctuations" and "Generalized CF", respectively.For comparison, the Gribov-Glauber model calculation with $\sigma = 25$ mb, which neglects the effect of CFs, is shown by the curve labeled "Glauber".

using the following procedure. For large $\sigma > \sigma_0$, we set $\sigma_{\rm eff} = \sigma$. For $\sigma < \sigma_0$, $\sigma_{\rm eff}$ is defined as the cross section corresponding to the gluon shadowing ratio $R_g(x)$ [44] calculated in the high-energy eikonal approximation:

$$R_g(x_{\rm eff}, Q^2_{\rm eff}) = \frac{x g_A(x_{\rm eff}, Q^2_{\rm eff})}{A x g_N(x_{\rm eff}, Q^2_{\rm eff})} = \frac{2}{A\sigma_{\rm eff}} \int d^2\vec{b} \left(1 - e^{-\sigma_{\rm eff} T_A(b)/2}\right) , \tag{12}$$

where $x_{\rm eff}$ and $Q^2_{\rm eff}$ are the light-cone momentum fraction and the resolution scale, respectively, which correspond to the dipole cross section for the given cross section $\sigma = \sigma_{q\bar{q}}(W, d_t, m_q)$ (the transverse size d_t), see Eq. (3). This prescription for $\sigma_{\rm eff}$ is based on the observation that since the non-vector-meson component of $P_\gamma(\sigma)$ is relatively small, the gluon shadowing can be considered in a simplified approximation, where CFs for the interaction with $N \geq 2$ nucleons are small and, hence, R_g is given by the single effective rescattering cross section $\sigma_{\rm eff}$.

To estimate the value of σ_0, we notice that the factor of nuclear suppression of coherent J/ψ photoproduction on nuclei is described very well for the LT nuclear shadowing. In particular, $R_g \approx 0.6$ for $x = 10^{-3}$ [47], which according to Eq. (12) corresponds to $\sigma_{\rm eff} = 17$ mb. Therefore, in our analysis we take $\sigma_0 = 20$ mb. Our numerical analysis indicates that the results of our calculation depend weakly on the method of smooth interpolation in Eq. (7) and the assumption about the value of the ratio $\sigma^{in}/\sigma^{in}_{\rm eff}$. We call the resulting approach to the calculation of photon–nucleus inelastic cross sections σ_ν the generalized color fluctuation (GCF) model. The result of the calculation of the distribution over ν using Eq. (11) is shown in Fig. 2 by the curve labeled "Generalized CF".

The results presented in Fig. 2 deserve a discussion. For one inelastic photon–nucleus interaction ($\nu = 1$), CFs in the photon lead to an almost a factor of two enhancement of $P(\nu)$ compared to the calculation neglecting CFs. Thus, an inclusion of the approximately 30% small-σ component of the photon wave function (see the discussion in the Introduction), leads to a large effect in the inelastic γA scattering. This effect is reduced approximately by a factor of two when we include the LT nuclear shadowing (compare the "Color Fluctuations" and "Generalized CF" curves). As ν increases, the small-σ contribution to the distribution $P_\gamma(\sigma, W)$ becomes progressively less important and all three models give similar results for $2 < \nu < 8$, where the contribution of the two terms in the integrand of Eq. (11) approximately compensate each other. For large $\nu > 10$, the two models including the effect of CFs in the photon predict a much broader distribution $P(\nu)$ than the model neglecting CFs: the enhancement at large ν comes from the contribution of the large-mass inelastic diffractive states implicitly included in Eqs. (9) and (11).

IV. COLOR FLUCTUATIONS AND THE DISTRIBUTION OVER TRANSVERSE ENERGY

It is impossible to directly measure the number of inelastic interactions ν for collisions with nuclei. Modeling the distribution over the hadron multiplicity is also difficult due to the lack of the relevant data from γp scattering and issues with implementing energy–momentum conservation. However, the analysis of [15] suggests that the distribution over the total transverse energy, ΣE_T, sufficiently far away from the projectile fragmentation region (at sufficiently large negative pseudorapidities) is weakly influenced by energy conservation effects (due to the approximate Feynman scaling in this region) and is also weakly correlated with the activity in the rapidity-separated forward region. This expectation is validated by a recent measurement of ΣE_T as a function of hard scattering kinematics in pp collisions at the LHC [48].

Due to the weak sensitivity to the projectile fragmentation region, we expect that the ΣE_T distributions in pA and γA scattering at similar energies should have similar shapes for the same ν. In Ref. [15], a model was developed for the distribution over ΣE_T as a function of centrality in pA scattering at large negative pseudorapidities (in the Pb-going direction) and $\sqrt{s} = 5.02$ TeV. In our discussion below, using the one-to-one correspondence between centrality and ν, we denote this distribution $f_\nu(\Sigma E_T) = 1/N_{\rm evt} dN/d\Sigma E_T$. In the spirit of the KNO scaling, it is natural to expect that the distribution over the ΣE_T total transverse energy in γA scattering, when normalized to the average energy release in pp scattering $\langle \Sigma E_T(NN) \rangle$, weakly depends on the incident collision energy. That is, the distribution over $y = \Sigma E_T(\gamma N)/\langle \Sigma E_T(\gamma N) \rangle$ has approximately the same shape at different energies. Hence we model the distribution over y for photon–nucleus collisions using $F_\nu(y) = \langle \Sigma E_T(NN) \rangle f_\nu(y)$, where the factor of $\langle \Sigma E_T(NN) \rangle$ is a Jacobian to keep normalization of $\int F_\nu(y) dy = P(\nu)$.

The results of the calculation of $F_\nu(y)$ are presented in Fig. 3 for the Generalized Color Fluctuations (GCF) model showing contributions of events with different ν to the normalized distribution over y. We separately show the contributions corresponding to $\nu = 1$, 2, 3, and 4, and the total contribution corresponding to the sum over all ν (the curve labeled "Total"). One can see that the net distribution is predicted to be much broader than that for the $\nu = 1$ case corresponding to the γp scattering. Also, our results indicate that for $y = \Sigma E_T(\gamma N)/\langle \Sigma E_T(\gamma N) \rangle \leq 1$, the contribution of the interactions with one nucleon dominates. On the other hand, the distribution over y in γp scattering can be measured in pA UPCs. A first step would be to test that the y distribution in γp and in the γA process with $\nu = 1$ [for example, in the interaction of the direct photon ($x_\gamma = 1$) with a gluon with $x_A \geq 0.01$] is the same. Among other things this would give a valuable information on the rapidity range affected by cascade interactions of slow (in the nucleus rest frame) hadrons which maybe formed inside the nucleus.

Next one would be able to compare the rates of $y < 1$ events in γp and γA to determine the fraction of the $\nu = 1$ and $\nu > 1$ events, which is quite sensitive to the model, see Fig. 2. One can see that for a given y, a range of ν

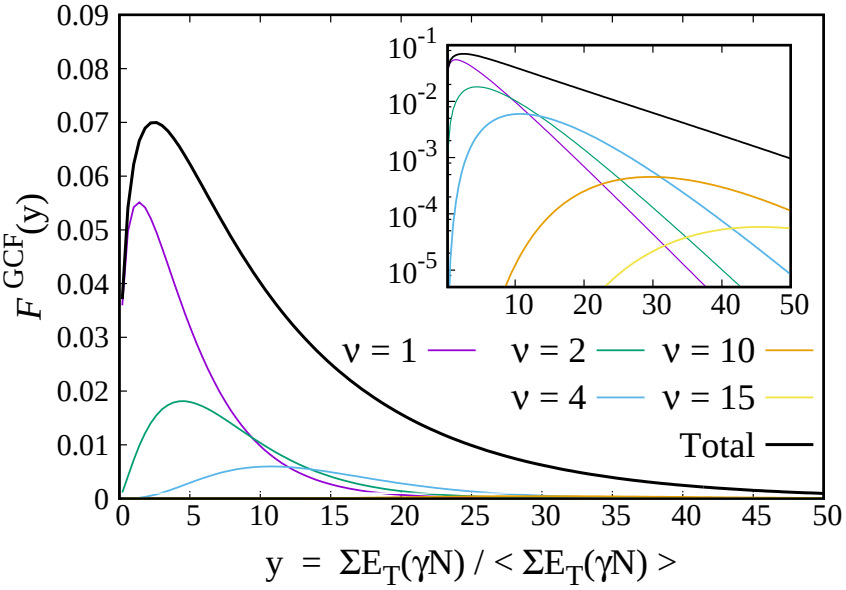

FIG. 3: The probability distributions $F_\nu(y)$ over $y = \Sigma E_T(\gamma N)/\langle \Sigma E_T(\gamma N) \rangle$ for different numbers of inelastic interactions ν in the Generalized Color Fluctuations (GCF) model.

contributes into the cross section. To a good approximation, $\langle \nu \rangle - 1 \propto y$. For $y = 10$, $\langle \nu \rangle$ reaches 2.8 (2.6, 3.1) for

the GCF (CF, Glauber) model with the variance typically of about ~ 0.15. The resulting smearing over ν for given y does not wipe out the difference between the models for the ν distribution, see Fig. 4.

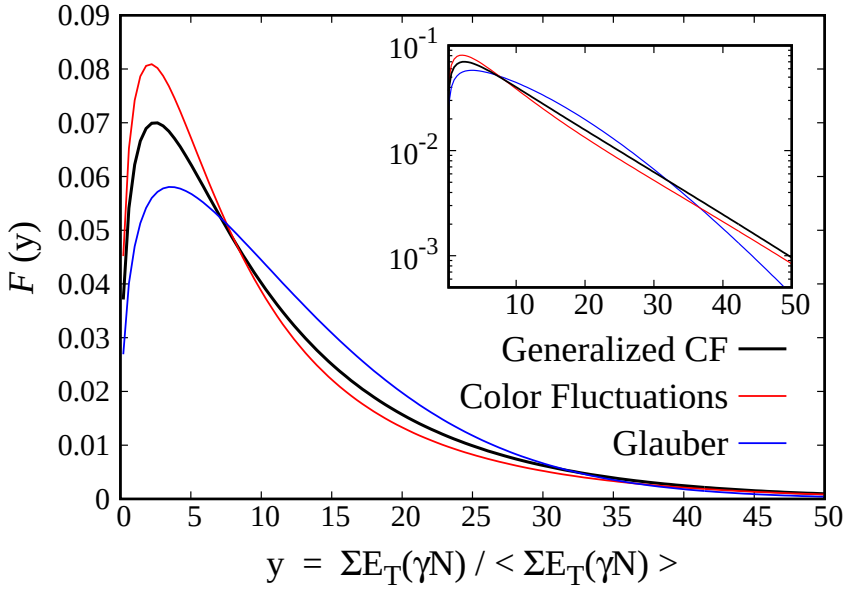

FIG. 4: The net probability distribution $\sum_\nu F_\nu(y)$ as a function of y for different models including (curves labeled "Generalized CFs" and "Color Fluctuations") and neglecting (the curve labeled "Glauber") CFs in the photon.

Since the distribution $F(y)$ is predicted to be much broader in γA collisions than in γp scattering, the use of different forward triggers makes it possible to determine the distribution over ν and use it to determine both $\langle\sigma\rangle$ and the variance of the $P_\gamma(\sigma, W)$ distribution for selected configuration. For example, in the CF model of Eq. (9) (*cf.* [9, 18]), which does not include the LT shadowing effects, one obtains the following relations for the average number of inelastic collisions $\langle\nu\rangle$,

$$\langle\nu\rangle = \frac{A\sigma_{in}(\gamma N)}{\sigma_{in}(\gamma A)}\,, \tag{13}$$

and for the variance of the cross section for a specific trigger,

$$\frac{\langle\sigma^2_{trig}\rangle}{\langle\sigma_{trig}\rangle} = \frac{(\langle\nu^2\rangle\,/\,\langle\nu\rangle - 1)\frac{A^2}{A-1}}{\int d^2b\, T_A^2(b)}\,. \tag{14}$$

Obviously similar considerations are applicable for the γA interactions with a special trigger including jet production, production of charm, etc. In the case of forward dijet production, for direct photon for $x_A \leq 0.01$, the leading twist shadowing should set in resulting in a broader distribution over ν as compared to the interactions with $x_A > 0.01$ (corresponding to $\nu = 1$), see the discussion in sections 6.3 and 6.4 of [44]. For the resolved photons, the distribution over ν (and hence over ΣE_T) should become broader with an decrease of x_γ since hadronic configurations with smaller x_γ have a larger transverse size. One also expects that for sufficiently small $x_\gamma < 0.1$, the hard process would select generic configurations in the photon and, hence, the distribution over ΣE_T would approach the distribution for generic (without trigger) γA collisions. Note that first studies of diffractive dijet photoproduction in pp, pA and AA UPCs at the LHC in next-to-leading order (NLO) QCD, where CFs in the photon were used to model the effect of factorization breaking, were reported in [49].

In the case of production of leading charm, small-size dipoles dominate (the variation of the transverse size is regulated by m_c and $p_t(charm)$), which allows one to study leading twist shadowing effects in the charm channel. For instance, for $x \sim 10^{-3}$, one expects $\langle\nu\rangle \sim 2$ and the corresponding reduction of $\sigma_{in}^{charm}(\gamma A)/A\sigma_{in}^{charm}(\gamma p)$, see Eq. (13).

V. CONCLUSIONS

In this paper, we quantify the general property of photon–hadron interactions at high energies that the photon can be viewed as a superposition of configurations interacting with different cross sections, which we call the phenomenon of color fluctuations (CFs), and propose a model for the distribution $P_\gamma(\sigma, W)$ describing these CFs. Using this model and also additionally taking into account the effect of leading twist nuclear shadowing for small-σ configurations, we for the first time give predictions for the distribution over the number of inelastic interactions ν in photon–nucleus scattering. Our results show that CFs lead to a dramatic enhancement of this distribution at the small $\nu = 1$ and the large $\nu > 10$ compared to the combinatorics familiar from the Glauber model. We also study the effect of CFs on the total transverse energy ΣE_T released in inelastic γA scattering with different triggers and point to specific indications of the CF effect. Our predictions can be tested in the photon–nucleus (γA) interactions in UPCs of ions at the LHC, which are characterized by high-intensity fluxes of quasi-real photons in a wide energy spectrum and which can be viewed as an effective "strengthonometor" of the different components of the photon wave function.

It would also allow one to obtain (using central tracking of the LHC detectors) unique information on the centrality dependence of the production of forward hadrons carrying a large fraction of the photon momentum ($x_F \geq 0.5$). For soft interactions, experiments at fixed-target energies did indicate a strong suppression of the low-p_t and large-x_F hadron production. At the same time, very little experimental information is available on suppression of the leading hadron production at the collider energies and on its W dependence. These and other related topics will be discussed in more detail elsewhere.

An alternative approach of [50] assumed the dominance of the single Pomeron exchange in the crossed channel, which branches into many Pomerons interacting with nucleons of nuclei. This approach predicts absence of the depletion of the yield of leading hadrons in high energy hadron–nucleus collisions. Hence, it is in variance with the existing data, see e.g. [51]. The physics of the Pomeron branching may become important at the energies significantly exceeding energies achieved at UPCs and at future eA collider, which are the subject of this paper.

Acknowledgments

L.F.'s and M.S.'s research was supported by the US Department of Energy Office of Science, Office of Nuclear Physics under Award No. DE-FG02-93ER40771.

[1] V. N. Gribov, Sov. J. Nucl. Phys. **9** (1969) 369 [Yad. Fiz. **9** (1969) 640].
[2] V. N. Gribov, hep-ph/0006158.
[3] T. H. Bauer, *et al.*, Rev. Mod. Phys. **50**, 261 (1978) [Erratum-ibid. **51**, 407 (1979)].
[4] L. L. Frankfurt, G. A. Miller and M. Strikman, Ann. Rev. Nucl. Part. Sci. **44**, 501 (1994) [hep-ph/9407274].
[5] L. Frankfurt, V. Guzey and M. Strikman, J. Phys. G **27**, R23 (2001) [hep-ph/0010248].
[6] D. Dutta, K. Hafidi and M. Strikman, Prog. Part. Nucl. Phys. **69**, 1 (2013) [arXiv:1211.2826 [nucl-th]].
[7] S. Mandelstam, Nuovo Cim. **30**, 1148 (1963).
[8] V. N. Gribov, Sov. Phys. JETP **29**, 483 (1969) [Zh. Eksp. Teor. Fiz. **56**, 892 (1969)].
[9] M. Alvioli, L. Frankfurt, V. Guzey and M. Strikman, Phys. Rev. C **90**, 034914 (2014) [arXiv:1402.2868 [hep-ph]].
[10] G. Alberi and G. Goggi, Phys. Rept. **74** (1981) 1.
[11] M. L. Good and W. D. Walker, Phys. Rev. **120**, 1857 (1960).
[12] H. I. Miettinen and J. Pumplin, Phys. Rev. D **18**, 1696 (1978).
[13] L. Frankfurt, V. Guzey and M. Strikman, Phys. Rev. D **58**, 094039 (1998) [hep-ph/9712339].
[14] G. Baym, B. Blattel, L. L. Frankfurt, H. Heiselberg and M. Strikman, Phys. Rev. Lett. **67** (1991) 2946; Phys. Rev. C **52**, 1604 (1995) [nucl-th/9502038].
[15] G. Aad *et al.* [ATLAS Collaboration], Eur. Phys. J. C **76**, no. 4, 199 (2016) [arXiv:1508.00848 [hep-ex]].
[16] L. Bertocchi and D. Treleani, J. Phys. G **3**, 147 (1977).
[17] V. Guzey and M. Strikman, Phys. Lett. B **633**, 245 (2006) [Phys. Lett. B **663**, 456 (2008)] [hep-ph/0505088].
[18] M. Alvioli and M. Strikman, Phys. Lett. B **722**, 347 (2013) [arXiv:1301.0728 [hep-ph]].
[19] G. Aad *et al.* [ATLAS Collaboration], Phys. Lett. B **748**, 392 (2015) [arXiv:1412.4092 [hep-ex]].
[20] A. Adare *et al.* [PHENIX Collaboration], Phys. Rev. Lett. **116**, no. 12, 122301 (2016) [arXiv:1509.04657 [nucl-ex]].
[21] M. Alvioli, B. A. Cole, L. Frankfurt, D. V. Perepelitsa and M. Strikman, Phys. Rev. C **93**, no. 1, 011902 (2016) [arXiv:1409.7381 [hep-ph]].
[22] J. Adam *et al.* [ALICE Collaboration], JHEP **1509**, 095 (2015) [arXiv:1503.09177 [nucl-ex]].
[23] L. Frankfurt, V. Guzey, M. Strikman and M. Zhalov, Phys. Lett. B **752**, 51 (2016) [arXiv:1506.07150 [hep-ph]].
[24] A. J. Baltz *et al.*, Phys. Rept. **458**, 1 (2008) [arXiv:0706.3356 [nucl-ex]].

[25] A. Accardi *et al.*, arXiv:1212.1701 [nucl-ex].
[26] D. Boer *et al.*, arXiv:1108.1713 [nucl-th].
[27] G. Altarelli, R. D. Ball and S. Forte, Nucl. Phys. B **621** (2002) 359 [hep-ph/0109178].
[28] V. Guzey, M. Strikman and M. Zhalov, Eur. Phys. J. C **74**, no. 7, 2942 (2014) [arXiv:1312.6486 [hep-ph]].
[29] V. N. Gribov, Sov. Phys. JETP **30**, 709 (1970) [Zh. Eksp. Teor. Fiz. **57**, 1306 (1969)].
[30] J. J. Sakurai, Annals Phys. **11**, 1 (1960).
[31] R. P. Feynman, *Photon-hadron interactions*, (Benjamin, Reading 1972), 282 p.
[32] J. D. Bjorken, Conf. Proc. C **710823**, 281 (1971).
[33] L. L. Frankfurt and M. I. Strikman, Phys. Rept. **160**, 235 (1988).
[34] B. Z. Kopeliovich and L. I. Lapidus, Pisma Zh. Eksp. Teor. Fiz. **28** (1978) 664.
[35] B. Blaettel, *et al.*, Phys. Rev. D **47**, 2761 (1993).
[36] L. Frankfurt, A. Radyushkin and M. Strikman, Phys. Rev. D **55**, 98 (1997) [hep-ph/9610274].
[37] M. McDermott, L. Frankfurt, V. Guzey and M. Strikman, Eur. Phys. J. C **16**, 641 (2000) [hep-ph/9912547].
[38] B. Blaettel, G. Baym, L. L. Frankfurt and M. Strikman, Phys. Rev. Lett. **70**, 896 (1993); L. Frankfurt, G. A. Miller and M. Strikman, Phys. Lett. B **304**, 1 (1993).
[39] L. Frankfurt, M. McDermott and M. Strikman, JHEP **0103**, 045 (2001) [hep-ph/0009086].
[40] N. N. Nikolaev and B. G. Zakharov, Z. Phys. C **49**, 607 (1991).
[41] K. A. Olive *et al.* [Particle Data Group Collaboration], Chin. Phys. C **38**, 090001 (2014).
[42] T. J. Chapin *et al.*, Phys. Rev. D **31**, 17 (1985).
[43] V. N. Gribov, Sov. Phys. JETP **26** (1968) 414 [Zh. Eksp. Teor. Fiz. **53** (1967) 654].
[44] L. Frankfurt, V. Guzey and M. Strikman, Phys. Rept. **512**, 255 (2012) [arXiv:1106.2091 [hep-ph]].
[45] B. Abelev *et al.* [ALICE Collaboration], Phys. Lett. B **718**, 1273 (2013) [arXiv:1209.3715 [nucl-ex]].
[46] E. Abbas *et al.* [ALICE Collaboration], Eur. Phys. J. C **73**, no. 11, 2617 (2013) [arXiv:1305.1467 [nucl-ex]].
[47] V. Guzey, E. Kryshen, M. Strikman and M. Zhalov, Phys. Lett. B **726**, 290 (2013) [arXiv:1305.1724 [hep-ph]].
[48] G. Aad *et al.* [ATLAS Collaboration], Phys. Lett. B **756**, 10 (2016) [arXiv:1512.00197 [hep-ex]].
[49] V. Guzey and M. Klasen, JHEP **1604**, 158 (2016) [arXiv:1603.06055 [hep-ph]].
[50] O. V. Kancheli, Pisma Zh. Eksp. Teor. Fiz. **18** (1973) 465 [JETP Lett. **18** (1973) 274].
[51] J. Adams *et al.* [STAR Collaboration], Phys. Rev. Lett. **97** (2006) 152302, [arXiv:nucl-ex/0602011].